Journal of Biosciences and Medicines, 2026, 14(1), 212-226
https://www.scirp.org/journal/jbm
ISSN Online: 2327-509X
ISSN Print: 2327-5081

In Silico ADMET, Molecular Docking of Antimicrobial Compounds from Leaves of *Xeroderris stuhlmannii* (Taub.) Mendonca & E.P. Sousa (*Fabaceae*)

Livie Blondele Kenou Mekuete[1*], Maraf Mbake Mbah[2], Hans Merlin Tsahnang Fofack[3], Yolande Noëlle Djouatsa Nangue[4], Donald Raoul Tchuifon Tchuifon[5], Anatole Guy Blaise Azebaze[4]

[1]Pole of Research, Innovation and Entrepreneurship, Institut Universitaire de la Cote, Douala, Cameroon
[2]Computational Chemistry Laboratory, Department of Chemistry, Higher Teacher Training College, University of Yaoundé I, Yaoundé, Cameroon
[3]Laboratoire Optique et Applications, Centre de Physique Atomique Moléculaire et Optique Quantique, Faculté des Sciences, Université de Douala, Douala, Cameroon
[4]Department of Chemistry, Faculty of Sciences, University of Douala, Douala, Cameroon
[5]Department of Process Engineering, Laboratory of Chemical Engineering and Industrial Bioprocesses, National Polytechnic School of Douala, University of Douala, Douala, Cameroon
Email: *livie.kenou@myiuc.com, *kenoulivie14@gmail.com

How to cite this paper: Kenou Mekuete, L.B., Mbah, M.M., Fofack, H.M.T., Nangue, Y.N.D., Tchuifon Tchuifon, D.R. and Azebaze, A.G.B. (2026) *In Silico* ADMET, Molecular Docking of Antimicrobial Compounds from Leaves of *Xeroderris stuhlmannii* (Taub.) Mendonca & E.P. Sousa (*Fabaceae*). *Journal of Biosciences and Medicines*, **14**, 212-226.
https://doi.org/10.4236/jbm.2026.141017

Received: November 5, 2025
Accepted: January 13, 2026
Published: January 16, 2026

Abstract

Xeroderris stuhlmannii is a plant that has been used for a long time in Cameroon and in Africa for the treatment of various diseases including: digestives disorders, diabetes, hypertension and skin infections. Four isolated compounds from the leaves' crude extract were chosen based on their antimicrobial activity reported in our previous work against *Escherichia coli*, *Staphylococcus aureus*, *Klebsiella pneumonae* and *Candida albicans*. **Materials and Methods:** Molecular docking calculations were made by AutoDock Vina software and the docking studies were performed with the same strains, while ADMET values were predicted by QikProp. 3D and 2D interaction with bacterial and fungal complexes are shown. **Results:** Based on the overall observations, we noticed that compounds bearing prenyl or geranyl groups at the C-7 or C-4' position exhibited high docking scores and interactions than those lacking such substituents. Undeniably, these substituents are decisive contributor to CYP51 inhibition, which promotes strong hydrophobic occupation of the active site and then facilitating interaction with the heme group. WF_{54} scaffold fits the hydrophobic pocket of DHFR, accounting for its potent antibacterial effect, while the isoflavone skeleton of NKL_8 is structurally aligned with the

geometry of DNA gyrase ATP binding pocket, which enables it to form a vast network of hydrogen and electrostatic bonds that disrupts ATP hydrolysis.

Keywords

Xeroderris stuhlmannii, Antimicrobial, ADME-Predictions, Molecular Docking

1. Introduction

Infectious diseases are a major global health problem of the 21st century that affects up to 2 million deaths each year [1]. The global surge in antimicrobial resistance has intensified the search for novel therapeutic agents, particularly those derived from medicinal plants with ethnopharmacological significance. Over the last decades, natural products have been found to possess diverse active compound(s) with interesting activities against microbes and many other diseases [2]. Up to date, computational investigation techniques have been used to evaluate the inhibitory potential of phytocompounds against G-positive and G-negative bacteria not microbes since microbes refers to bacteria, fungi, viruses [3] [4]. Several studies have proven the antioxidant, antidiabetic potential of prenylated flavonoids compounds in plants to treat microbial diseases [5]-[8]. Microbial diseases in humans commonly affect the digestive tube due to the fact that people are exposed to long treatment several times. However, the control and the eradication programs have been marked by some lapses of stagnation and relapse.

Xeroderris stuhlmannii is a Cameroonian medicinal plant widely use for the treatment of many affections including inflammations, infectious diseases and more specifically the gastrointestinal disorders [8]-[11]. The phytochemical works done on the leaves revealed the in vitro antibacterial potential of some isolated phenolic compounds. The preliminary results obtained show that the different substituents and positions such as prenyl groups, furan group, hydroxylation and methylation give different values in terms of biological activities compared to their non-substituted analogue [8]. Despite its widespread use in traditional pharmacopeia, the phytochemical constituents of its leaves remain underexplored through modern drug discovery pipelines.

Recent advances in computational biology have enabled the rapid screening of plant-derived compounds using *in silico* techniques such as ADMET (Absorption, Distribution, Metabolism, Excretion, and Toxicity) profiling and molecular docking. ADMET analysis predicts the pharmacokinetic behavior and safety of candidate molecules, while docking simulations assess their binding affinity and interaction with microbial targets, offering insights into potential mechanisms of action. These approaches have been successfully applied to other medicinal plants, demonstrating their utility in identifying promising antimicrobial agents [10] [12]-[20]. *In silico* and docking studies have proven their effectiveness in identifying novel remedies

that offer ideally all the requirements as anti-infectious agents. In light to this situation, it is therefore crucial to perform the investigation of *Xeroderris stuhlmannii* through in silico approaches. The *in silico* investigations such as drug-likeness properties, pharmacokinetics and the molecular docking studies of the isolated compounds from *Xeroderris stuhlmannii* should be addressed. Among the diverse classes of phytochemicals, prenylated compounds characterized by the addition of hydrophobic prenyl groups have garnered attention for their enhanced biological activity. Prenylation increases lipophilicity, improves membrane permeability, and often strengthens binding interactions with target proteins, thereby boosting antimicrobial potency. These structural modifications can also influence metabolic stability and bioavailability, making prenylated flavonoids, chalcones, and coumarins particularly attractive for drug development. This study investigates the antimicrobial potential of compounds isolated from the leaves of *X. stuhlmannii*, with a focus on prenylated bioactives constituents namely Conrauinone A, Conrauinone C, Stuhlmarotenoid A, 7-*O*-geranylformononetin [8]. Using *in silico* ADMET prediction and molecular docking simulations, we aim to identify promising lead compounds and elucidate their pharmacological profiles. By integrating traditional knowledge with computational modeling, this work contributes to the rational design of plant-based antimicrobial agents.

2. Materials and Methods

2.1. Target Protein Structure and Ligand Preparation

To investigate the antibacterial and antifungal properties of 04 selected molecules, molecular docking calculations were performed using Glide module [21] of the Schrödinger software suite (Schrödinger, LLC, New York, NY, 2023) using the extra precision (xp) mode [22]. The structure of compounds 1 - 4 were drawn using the 2D sketch panel of a Schrodinger and prepared using the Ligprep module (Schrödinger Release 2024-3, LigPrep, Schrödinger, LLC, New York, NY, 2024a) with OPLS force field [23], generating lower energy conformers and ionization states at pH 7.0 ± 2.0. The co-crystallized structures of the chosen receptors were retrieved from the Protein Data Bank (PDB) website (https://www.rcsb.org/pdb/) Lanosterol 14-*α*-demethylase (CYP51) from *candida albicans* (pdb id: 5TZ1, 2.0 Å), dihydrofolate reductase (DHFR) from *staphylococcus aureus* (pdb id: 3SRW, resolution 1.7 Å), and DNA gyrase subunit B (GyrB) from *Escherichia coli* (pdb id: 4DUH, resolution: 1.5 Å). These targets were selected for their established roles in fungal and bacterial viability and for alignment with the reported in vitro activity of *Xeroderris stuhlmannii* extracts. CYP51 is a key enzyme in ergosterol biosynthesis making it appropriate for antifungal evaluation [24] [25]. DHFR catalyzes the reduction of dihydrofolate to tetrahydrofolate and is a validated antibacterial target, notably for gram positive pathogens [26]. DNA gyrase mediates DNA supercoiling and is a canonical target for antibacterial agents active against gram negative organisms [25]. The protein structures were prepared using the protein preparation wizard of Schrödinger suite (Schrödinger Release 2024-4, Protein

Preparation Wizard; Epik, Schrödinger, LLC, New York, NY, 2024; Impact, Schrödinger, LLC, New York, NY; Prime, Schrödinger, LLC, New York, NY, 2024b). The preparation protocol involved: assigning of bond orders and addition of hydrogen, removal of water molecules beyond 5 Å from the native ligand, missing side chains and loops were modelled, protonation states were assigned using Epik at pH 7.0 ± 2.0, and structures were subjected to restrained minimization with OPLS4 force field. Receptor grids were generated centered on the coordinates of the co-crystallized ligands. Docking simulation was validated by redocking the native ligands into their respective active site. Validation success was determined by RMSD values between the docked and crystallographic pose, with RMSD < 2.0 Å considered acceptable [27].

2.2. Binding Free Energy Calculation (MMGBSA)

To refine the accuracy of the ligand, pose ranking and evaluate the thermodynamic stability and selectivity of the docked complexes, the binding free energies ΔGbind were computed by applying the prime Molecular Mechanics generalized Born Surface Area (MMGBSA) approach (Schrödinger Suite 2024 User Manual; Prime MM-GBSA Calculation Methodology and Solvation Models, Schrödinger, New York, NY). This method provides a more rigorous estimation of the binding energy compared to standard scoring functions by incorporating solvation effects. The binding free energies ΔGbind was determined from the output poses obtained from docking simulation using the following equations:

$$\Delta Gbind = \Delta G\ (complex) - (\Delta G\ (Protein) + \Delta G\ (Ligand) \quad (1)$$

The free energy, (for each component is estimated by the molecular mechanics energy (EMM), the solvation free energy (Gsolv) and the product of the absolute temperature (T) and entropy change (ΔS):

$$\Delta Gbind = \Delta EMM + \Delta Gsol - T\Delta S \quad (2)$$

2.3. ADMET

QikProp was used to determine the toxicity, bioavailability, and pharmacodynamic characteristics of 4 selected hits FAXD, WF_{54}, NKL_{19} and NKL_{8} isolated from *X. stuhlmannii*. The compounds were chosen based on factors such as Lipinski's rule of five (Ro5), gastrointestinal absorption, inhibition of CYP450 isoenzymes, hepatotoxicity, ocular irritation, corrosion, biodegradation, and others. Compounds that passed the drug-likeness screening were docked using the gliding docking techniques.

3. Results and Discussion

This paper discusses the results of a virtual screening protocol of four ligands to select the best hit compounds for experimental validation.

3.1. ADMET Screening

To prevent adverse ADMET features (absorption, distribution, metabolism, excre-

tion, and toxicity), pharmacokinetics and toxicity should be considered throughout the initial stages of drug development. The compounds potential druggability was estimated using QikProp. In this study, we first estimated the database's ADMET attributes. Table I shows the results for the 04 selected hits.

Indeed, Table 1 illustrates that ligands FAXD, NKL_8, NKL_{19}, AND WF_{54} (See Figure 1) exhibit favorable PHO, HOA, and QPPCaco permeability values, indicating good oral absorption and permeability. Notably, NKL_{19} has the lowest PSA, which supports enhanced membrane permeability and distribution. Based on the overall ADMET profiles, which rank the ligands from most to least likely to be good drug candidates FAXD and WF_{54} have high cell permeability, solubility, and oral absorption (PSA) contributing to good oral absorption; low PSA and high lipophilicity enable good distribution, low risk of cardiotoxicity; and show strong absorption and distribution properties. However, they show a slightly higher metabolism risk due to hydrophobic regions and low brain penetration. To summarize, both selected hits exhibit an optimal balance of drug likeness properties and ADME potential.

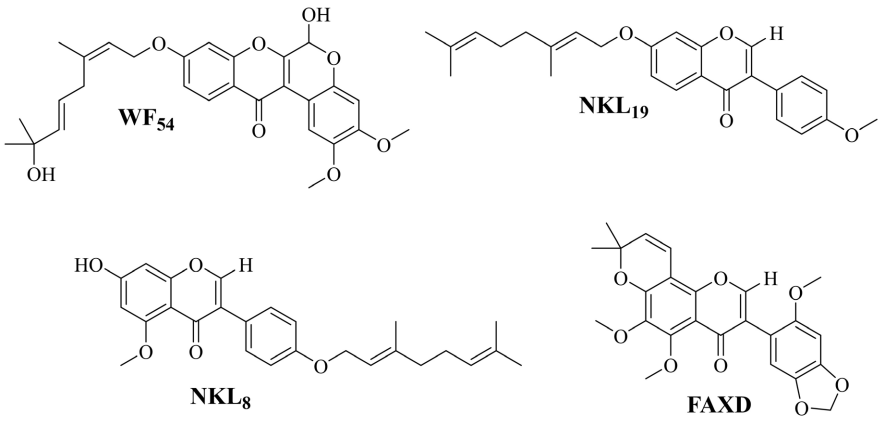

Figure 1. Chemical structures of the selected compounds for molecular docking studies.

Table 1. QikProp pharmacokinetic and toxicity predictions of selected ligands.

Ligand	SASA	FOSA	FISA	PISA	WPSA	$R_O3/5$	volume	donor HB	AccptHB	HOA	PHO	PSA	QplogS	CIQPlogS	QPlogHERG	QPPCaco	QPlogBB
FAXD	588.42	202.89	80.33	305.19	0		1021.28	0	5.75	3	100	59.52	−3.71	−6.44	−5.68	1714.38	−0.45
NKL_8	654.5	182.79	108.97	362.74	0		1098.37	0	4	3	100	61.82	−5.55	−6.69	−6.72	917.28	−0.97
NKL_{19}	657.18	262.29	64.48	330.42	0		1102.98	0	3.5	3	100	47.29	−5.7	−6.4	−6.58	2423.41	−0.56
WF_{54}	684.19	137.61	158.02	388.56	0		1174.07	0	8.5	3	84.39	103.11	−3.92	−6.24	−6.84	314.34	−1.44

SASA = Solvent Accessible Surface Area, FOSA = Hydrophobic component of SASA, FISA = Hydrophilic component of SASA, PISA = Pi (flat) component of SASA, WPSA = Total SASA excluding PISA, $R_O5/3$ = Role of Five/Three, Volume = Molecular volume, Donor HB = Estimated number of hydrogen bonds donated by the molecule, AccptHB = Estimated number of hydrogen bonds accepted by the molecule, HOA = Predicted human oral absorption on 0 - 3 scale, PHO = Percentage of oral absorption, PSA = Polar surface area, QplogS = Predicted aqueous solubility, CIQPlogS = Consensus log S (average of two prediction methods), QPlogHERG = Predicted IC_{50} value for blockage of HERG K+ channels, QPPCaco = Predicted apparent Caco-2 cell permeability, QPlogBB = Predicted brain/blood partition coefficient.

3.2. Molecular Docking Analysis

Molecular docking simulation was conducted to investigate the binding interactions of the isolated compounds with key microbial targets: fungal lanosterol 14-*α*-demethylase (PDB: 5TZ1), bacterial dihydrofolate reductase (DHFR, PDB: 3SRW), and bacterial DNA gyrase subunit B (GyrB, PDB: 4DUH). The binding affinities were evaluated using docking score, XP score, Glide score, with more robust binding energy estimates provided by the MMGBSA calculations (Table 2). To ensure the reliability of the docking procedure, redocking of each receptor's native ligand was performed, and the resulting RMSD superimposition values were all below 2 Å (Figure 2).

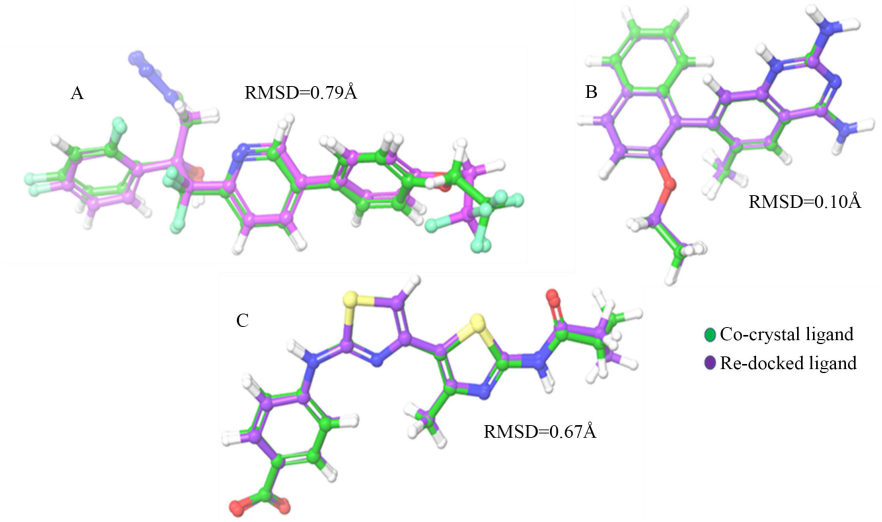

Figure 2. Redocking superimposition of Cocrystal ligand of (A) 5TZ1, (B) 3RSW, and (C) 4DUH.

Table 2. Docking score results of compounds.

Ligands	Docking score	XP GScore	Glide GScore	MMGBSA dG Bind
		5TZ1		
WF_{54}	−9.482	−9.482	−9.482	−40.10
NKL_{8}	−10.392	−10.392	−10.392	−37.57
NKL_{19}	−10.131	−10.131	−10.131	−33.32
FAXD	−7.408	−7.408	−7.408	−11.99
NYSTATIN	−8.038	−8.038	−8.038	−23.26
		3SRW		
WF_{54}	−7.637	−7.637	−7.637	−61.39
NKL_{8}	−6.890	−6.890	−6.890	−57.20
NKL_{19}	−3.147	−3.147	−3.147	−50.12
FAXD	−5.848	−5.848	−5.848	−48.83
NYSTATIN	−5.658	−5.658	−5.658	−56.86
CIPRO	−7.893	−7.893	−7.893	−47.13

Continued

	4DUH			
WF_{54}	−3.920	−3.920	−3.920	−43.20
NKL_8	−6.668	−6.668	−6.668	−54.52
NKL_{19}	−5.780	−5.780	−5.780	−51.74
FAXD	−4.376	−4.376	−4.376	−43.63
CIPRO	−6.904	−6.904	−6.904	−34.56

WF_{54} = Stuhlmarotenoid A; NKL_{19} = 7-*O* geranyl formononetin; NKL_8 = Conrauinone C and FAXD = Conrauinone A.

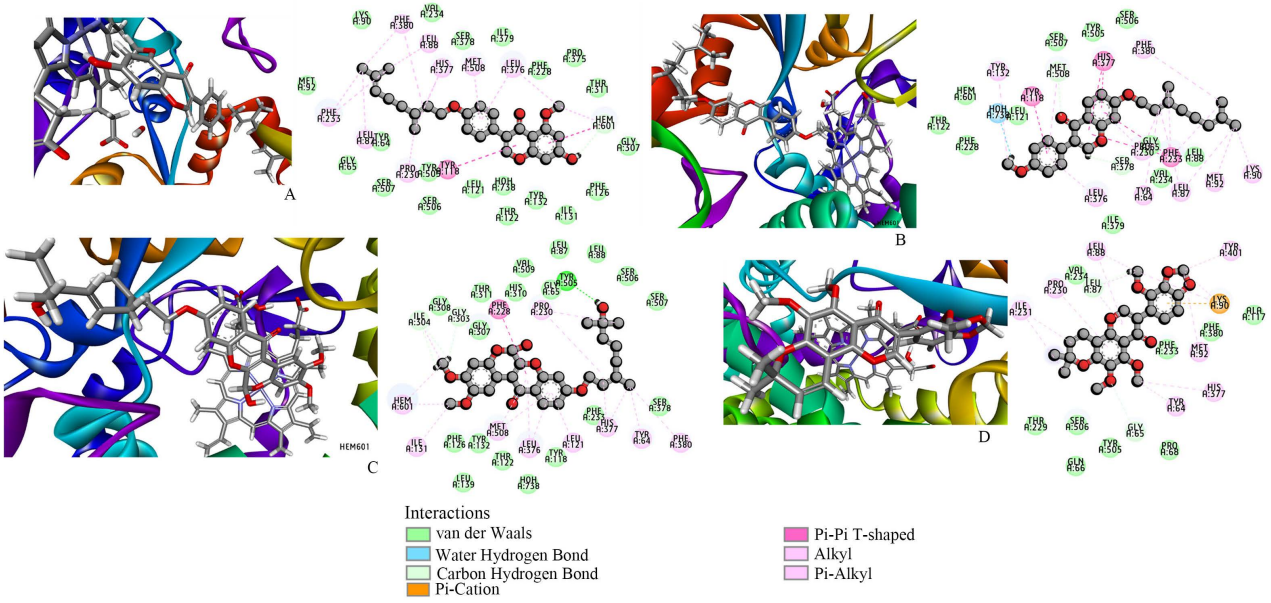

Figure 3. 3D pose view and 2D interaction map of fungal lanosterol 14-*α*-demethylase complexes (A) NKL_8-5TZ1, (B) NKL_{19}-5TZ1, (C) WF_{54}-5TZ1 and (D) FAXD-5TZ.

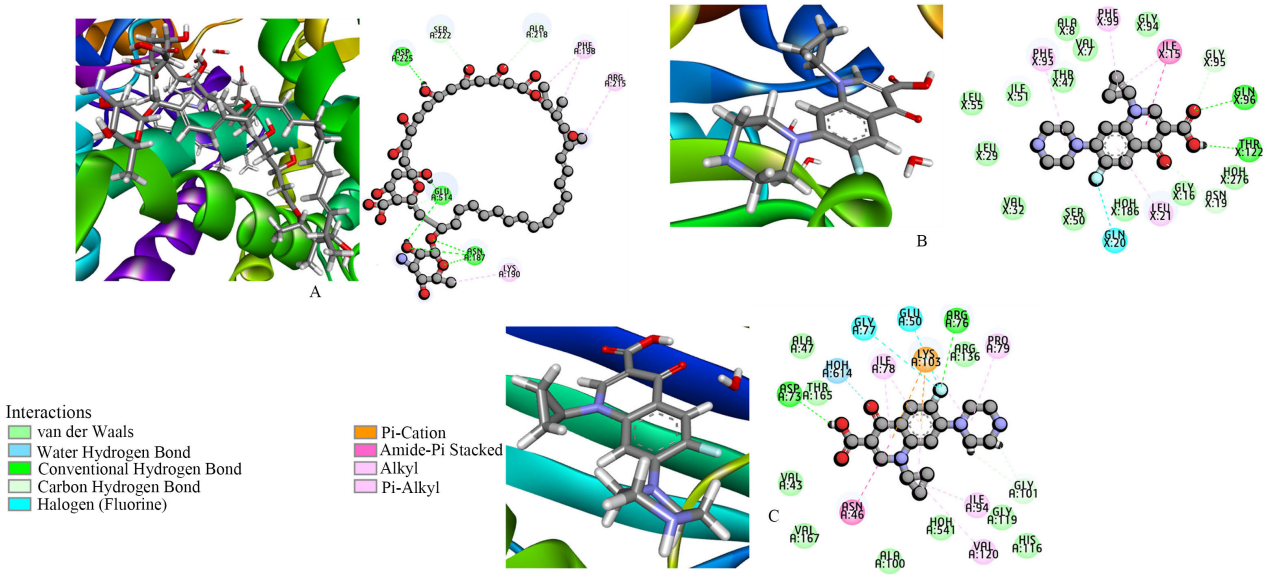

Figure 4. 3D pose view and 2D interaction map of (A) Nystatin-5TZ1, (B) Cipro-3SRW and (C) Cipro-4HUD.

3.2.1. Docking Interactions with Fungal Lanosterol 14-α-Demethylase

Docking against lanosterol 14-α-demethylase showed critical interactions with the Heme group and active cavity (**Figure 3**). The analysis of binding poses within the lanosterol 14-α-demethylase active site demonstrated distinct interaction profiles for each compound. Conrauinone C (NKL_8) exhibited a superior docking score of −10.392 Kcal/mol, forming a pi-pi T-shaped interaction and a pi-donor hydrogen bond with essential HEM601 group, alongside extensive pi-alkyl interactions with Met508, Phe380, His377, and Leu376 with the active site (**Figure 3(A)**). All those high interactions strongly support the fact that the geranyl moiety enhances the antibacterial activity of these compounds. Similarly, 7-*O*-geranylformononetin (NKL_{19}), showed a docking score of −10.131 kcal/mol, engaged in pi-pi T-shaped interactions with Tyr118, His377, and Phe233, a Van der Waals interaction with HEM601 group, and pi-alkyl interaction with Tyr132, Leu376, and Met508 (**Figure 3(B)**). Stuhlmarotenoid A (WF_{54}) exhibited a docking score of −9.482 kcal/mol. The compound directly engages the catalytic heme group through pi-pi T-shaped interactions and stabilizes its position in the active site via hydrogen bond with Tyr505 and a pi-pi T-shaped interaction with Phe228 (**Figure 3(C)**). In contrast, the binding mode of Conrauinone A (FAXD) with docking score −7.408 kcal/mol implies an alternative mechanism. Conrauinone A anchors itself within the active site through pi-cation interaction with Lys90, supported by extensive hydrophobic contacts (alkyl and pi-alkyl) with residues His377, Pro230, and Tyr64 (**Figure 3(D)**). The reduction in term of docking score in conrauinone A could be due to the replacement of the geranyl moiety by the 2,2-dimethylpyran substituents on ring A. The control drug Nystatin achieved binding through five hydrogen bonds with Asn187, Asp225, and Glu514 (**Figure 4(A)**).

3.2.2. Docking Interactions of Compounds with Bacterial Dihydrofolate Reductase (Dhfr)

Docking against DHFR shows that high binding affinity involves extensive hydrophobic contact in the active site. The docking results against DHFR revealed Stuhlmarotenoid A (WF_{54}) as top binder with docking score and MMGBSA score of −7.63 kcal/mol and −61.39 kcal/mol respectively. Its high affinity is driven by a hydrogen bond with Gln20 that anchors the molecule in DHFR active site, and extensive hydrophobic contacts across the wide surface of the binding pocket, engaging Leu29, Leu21, Val32, Lys33, Val7, Ile15, Phe99, and Pro26 (**Figure 5(A)**). The highest values observe with stuhlmarotenoid A is due to the important presence of methoxy group on almost all the cycle as compared to other compounds. NKL_8 exhibited a docking score and MMGBSA scores of −6.890 kcal/mol and −57 kcal/mol. The compound was stabilized in DHFR active through a conventional hydrogen bond with Th122. It was also observed to engage pi-alkyl interactions with as well as alkyl interactions with Lys30, Lys33, and Phe99 (**Figure 5(B)**). On the other hand, FAXD achieved a docking score of −5.848 kcal/mol and MMGBSA score of −48.83 kcal/mol. The ligand was stabilized in the active site through pi-alkyl interactions with residues Leu29, Leu55, Ile15, Phe99, and Phe93, comple-

mented alkyl interactions with Ile51, suggesting a predominantly hydrophobic stabilization with the active pocket (Figure 5(C)). Lastly, NKL_{19} showed a relatively weal affinity for DHFR (−3.147 kcal/mol), stabilized mainly by pi-alkyl interactions with Leu29, Leu55, Leu21, and Val32 (Figure 5(D)). Ciprofloxacin exhibited a well-defined binding mode, forming hydrogen bonds with Gln96 and Thr122, a halogen bond with Gln20, and hydrophobic interactions with Leu21, Phe93, Phe99, and Ile15 (Figure 4(B)).

3.2.3. Docking Interactions of Compounds with DNA Gyrase B

Docking against DNA-gyrase demonstrates that the inhibition correlates with disruption of the ATP-binding site through key electrostatic interactions (Figure 6). NKL_8 was the most potent achieving a docking score of −6.668 kcal/mol, forming a hydrogen bond with Asp73, pi-cation contact with Glu50, and an amide-pi stacked interaction with Asn46 (Figure 6(A)). FAXD also demonstrated a strong binding pose driven by three hydrogen bonds to Arg136 with Arg76 and Lys103, a pi-anion interaction with Glu50, as well as van der Waals with Asn46 (Figure 6(B)). NKL_{19} demonstrated a docking score of −5.780 kcal/mol. It exhibited a water mediated hydrogen bond, pi-cation contact with Arg76 and Lys103. It also displayed a pi-anion contact with Glu50, and Van der Waals contact with Asn46 (Figure 6(C)). WF_{54} (docking score −3.920 kcal/mol) interacted was stabilized through hydrogen bond with Arg136, pi-cation interaction with Arg76 and Lys103, pi-anion contact with Glu50 and lastly an amide-pi stacked with Asn46 (Figure 6(D)). Notably, several compounds consistently engaged ASN46, a residue that coordinates the catalytic Mg^{2+} required for ATP hydrolysis, indicating that ligand binding at this site may directly disrupt enzymatic activity [28] [29]. Ciprofloxacin reproduced the expected binding pattern, confirming docking reliability (Figure 4(C)).

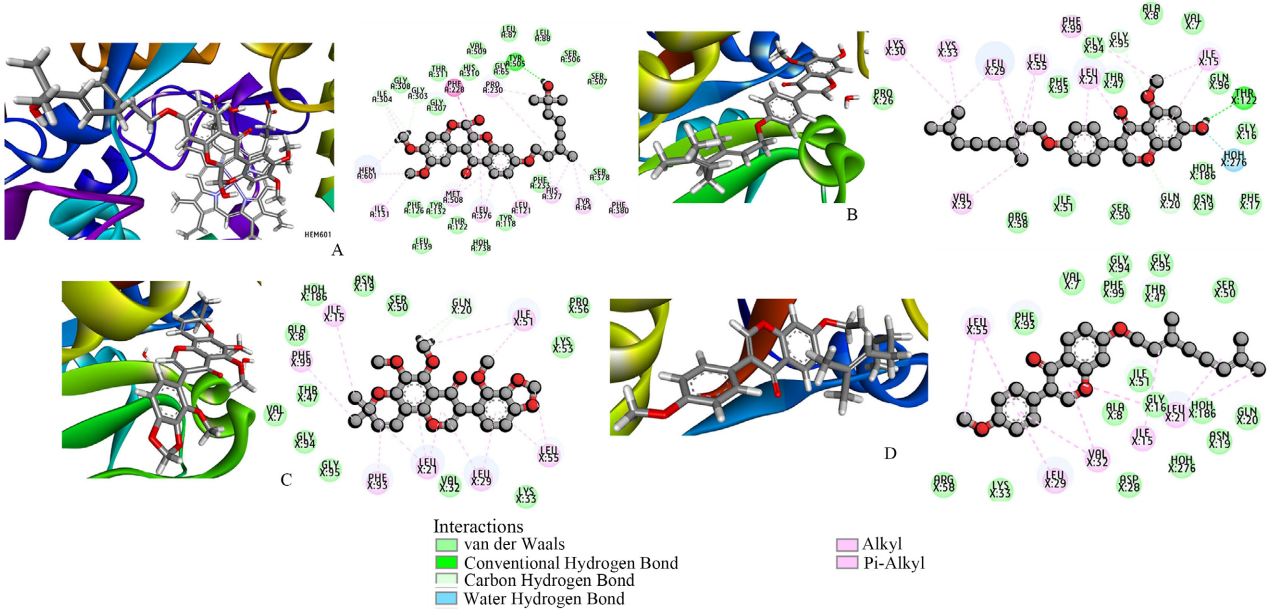

Figure 5. 3D pose view and 2D interaction map of bacterial dihydrofolate reductase complexes (A) WF_{54}-3SRW, (B) NKL_8-3SRW, (C) FAXD-3SRW, (D) NKL_{19}.

Table 3. Structure-activity relationship between non and prenylated compounds from *X. stuhlmannii*.

Bacteriostatic compounds (MBC/MIC > 4)	Bactericidal compounds (MBC/MIC ≤ 4)
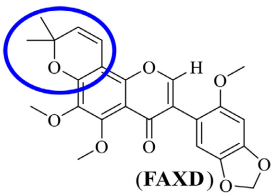 (FAXD) MIC = 62.5 µg/mL	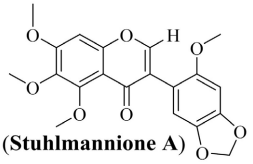 (Stuhlmannione A) MIC > 125 µg/mL 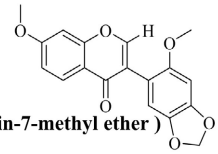 (cuneatin-7-methyl ether) MIC > 125 µg/mL
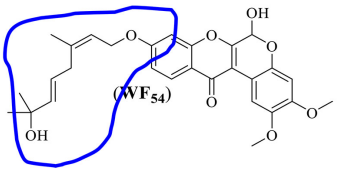 (WF_{54}) MIC = 62.5 µg/mL	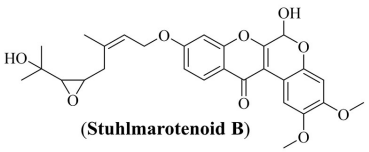 (Stuhlmarotenoid B) MIC > 125 µg/mL
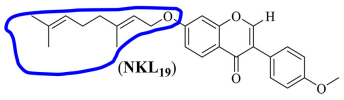 (NKL_{19}) MIC = 62.5 µg/mL 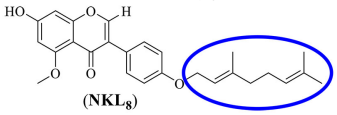 (NKL_8) MIC = 62.5 µg/mL	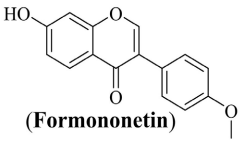 (Formononetin) MIC > 125 µg/mL

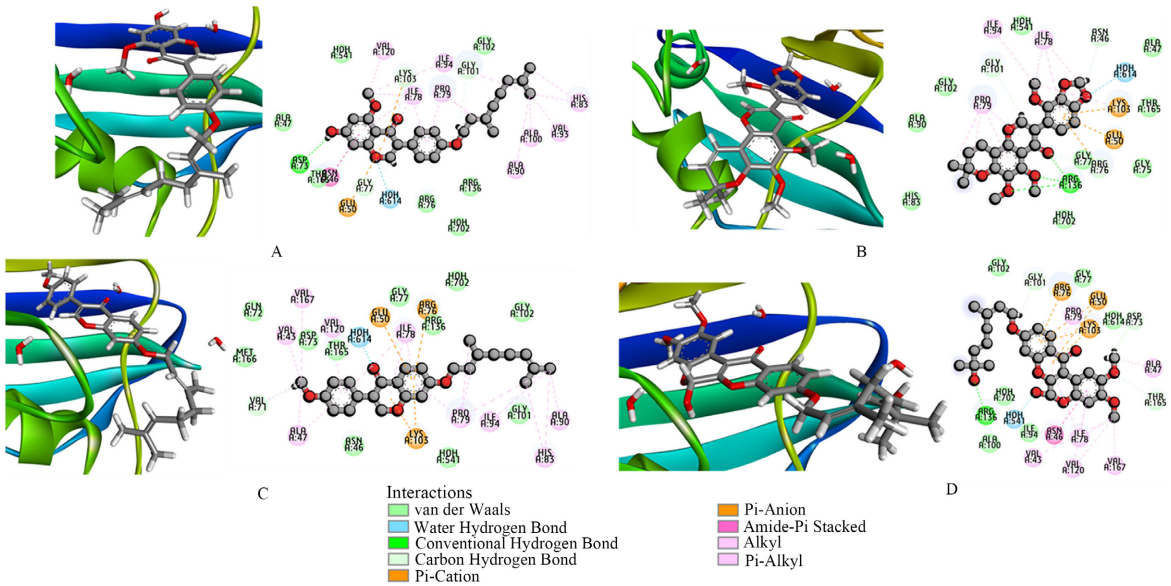

Figure 6. 3D poses view and 2D interaction map of bacterial DNA gyrase complexes (A) NKL_8-4HUD, (B) FAXD-4HUD, (C) NKL_{19}-4HUD, (C) WF_{54}-4HUD.

4. Discussion

The combined computational and experimental MIC data of prenylated and non-prenylated compounds (**Table 3**) yields a coherent structure-activity relationship in which the specific binding interactions provide a mechanistic explanation for the observed bioactivity. Overall observations were consistent with previous findings, indicating that compounds bearing prenyl, geranyl or geraniol groups at the C-7 or C-4' position exhibited significant antibacterial and antifungal activities than those lacking such substituents [8]. Indeed, the geranyl substituent is a decisive contributor to CYP51 inhibition, promoting strong hydrophobic occupation of the active site and, for the most active derivatives, facilitating interaction with the heme group. Stuhlmarotenoid A rotenoid scaffold fits the hydrophobic pocket of DHFR, accounting for its potent antibacterial effect. The isoflavone skeleton of Conrauinone C is structurally aligned with the geometry of DNA gyrase ATP binding pocket, allowing it to form an extensive hydrogen-bond and electrostatic network the perturbs ATP hydrolysis. The close correspondence between these precise molecular contacts heme group in CYP51, hydrophobic anchoring in DHFR and Mg^{2+} dependent Asn46 engagement in DNA gyrase and the MIC results offers strong mechanistic support for enzyme inhibition as key mode of action for the most active *X. stuhlmannii* metabolites. The binding affinity in almost all these compounds are likely due to the presence of the geranyl side chain or prenylation. The mechanism of action in MDR bacteria is based on the inhibitory effect on the efflux pump and the Hydrogen bonds participate in enhancing antibacterial activity. However, the low water solubility of the compounds is a pharmacokinetic disadvantage. All those information strongly supports the chemotaxonomy membership of *Xeroderris stuhlmannii* to the Fabaceae family and also by the activity reported on prenylated isoflavones and rotenoid with antibacterial activity.

By integrating docking simulation and ADMET profiling, we enhance early prioritization of lead candidates by combining target engagement and predicted pharmacokinetics. Compounds FAXD and WF_{54}, identified as the best results of the QikProp analysis due to the their favorable ADMET profiles, also display competitive binding affinities across targets. WF_{54} demonstrated the strongest interaction with DHFR (docking score: −7.63 kcal·mol^{-1} and MMGBSA: −61.39 kcal·mol^{-1}). The strength of this affinity is attributed to its rotenoid skeleton, which fits well into the hydrophobic pocket of DHFR. WF_{54} equally possesses excellent predicted absorption properties, as indicated by its high predicted oral absorption (PHO: 83.39%) and good Caco-2 permeability (QPPCaco: 314.34 nms-1). However, its relatively high polar surface area (PSA: 103.11 Å2) and low predicted brain-blood partition coefficient (QPlogBB: −1.44) collectively indicate reduced blood brain barrier penetration. This ADME profile favors its distribution towards peripheral tissues rather than central nervous system (CNS).

Furthermore, FAXD exhibits strong binding to DNA gyrase B (strong hydrogen bonds with Arg136 and Arg76), which complements its low cardiotoxicity and

good distribution predicted by ADMET. In contrast, NKL_8 and NKL_{19}, although excellent in terms of binding to fungal CYP51 (NKL8: −10.392 kcal/mol), have moderately less optimal metabolic profiles, suggesting potential for structural modifications to improve bioavailability. These synergies highlight that FAXD and WF_{54} are priority candidates for further *in vivo* validation, as the computational power is supported by drug-like properties.

Despite the fact that this *in silico* study provides valuable information on the antimicrobial potential of *X. stuhlmannii* compounds, several limitations inherent to computational approaches must be considered. Both molecular docking and the MMGBSA method rely on static protein structures, which may not fully reflect conformational dynamics or *in vivo*-induced fitting effects [30]. Scoring functions, although validated (RMSD < 2 Å), are approximations and may overestimate or underestimate affinities due to simplified solvation models and the neglect of explicit entropy changes [31]. QikProp ADMET Predictions are based on empirical modelling and may not account for species-specific metabolism or off-target effects [32]. Furthermore, the study focuses on selected targets, which may lead to the neglect of other mechanisms of action. Such limitations highlight the need for experimental validation through *in vitro* enzyme inhibition assays, cellular uptake studies, and *in vivo* pharmacokinetic studies to confirm predicted profiles and resolve potential discrepancies [33].

5. Conclusion

X. stuhlmannii is well known for its potentials against digestive disorders, skin problem, hypertension and diabetes. The present study focused on the *in silico* molecular docking studies of phytocompounds isolated from leaves of *X.s*. Collectively, all the promising results from QikProp analysis, binding affinity and Docking profile of the 4 phytocompounds (Stuhlmarotenoid A; 7-*O* geranyl formononetin; Conrauinone C and Conrauinone A) previously isolated from a Cameroonian plant reported in this study reveal that either FAXD or WF_{54} could serve as therapeutic agents against fungal and bacterial infections. However, the in vivo studies would have to be carried out to validate our findings.

Acknowledgements

The authors are thankful for the facilities provided by the University of Douala during the calculations.

Conflicts of Interest

The authors declare that they have no conflicts of interest regarding this work or the publication of this paper.

References

[1] Powell, H., Liang, Y., Neuzil, K.M., Jamka, L.P., Nasrin, D., Sow, S.O., *et al.* (2023) A Description of the Statistical Methods for the Vaccine Impact on Diarrhea in Africa

(VIDA) Study. *Clinical Infectious Diseases*, **76**, S5-S11. https://doi.org/10.1093/cid/ciac968

[2] Boozari, M., Soltani, S. and Iranshahi, M. (2019) Biologically Active Prenylated Flavonoids from the Genus *Sophora* and Their Structure-Activity Relationship—A Review. *Phytotherapy Research*, **33**, 546-560. https://doi.org/10.1002/ptr.6265

[3] Prabha, S. and Rayan, B.A. (2022) *In Silico* Analysis of Selected Compounds Using Pass. *International Journal of Scientific Development and Research*, **7**, 542-546.

[4] Xiong, G., Wu, Z., Yi, J., Fu, L., Yang, Z., Hsieh, C., *et al.* (2021) ADMETlab 2.0: An Integrated Online Platform for Accurate and Comprehensive Predictions of ADMET Properties. *Nucleic Acids Research*, **49**, W5-W14. https://doi.org/10.1093/nar/gkab255

[5] Balida, L.A.P., Regalado, J.T.A., Teodosio, J.J.R., Dizon, K.A.H., Sun, Z., Zhan, Z.Q., *et al.* (2022) Antibiotic Isoflavonoids, Anthraquinones, and Pterocarpanoids from Pigeon Pea (*Cajanus cajan* L.) Seeds against Multidrug-Resistant *Staphylococcus aureus*. *Metabolites*, **12**, Article 279. https://doi.org/10.3390/metabo12040279

[6] Faraone, I., Rai, D.K., Chiummiento, L., Fernandez, E., Choudhary, A., Prinzo, F., *et al.* (2018) Antioxidant Activity and Phytochemical Characterization of Senecio Clivicolus Wedd. *Molecules*, **23**, Article 2497. https://doi.org/10.3390/molecules23102497

[7] Selemani, M.A., Kazingizi, L.F., Manzombe, E., et al. (2020) Phytochemical Characterization and *in Vitro* Antibacterial Activity of *Xeroderris stuhlmannii (Taub.)* Mendonca & E.P. Sousa Bark Extracts. *South African Journal of Botany*, **142**, 344-351.

[8] Mekuete, L.B.K., Tsopgni, W.D.T., Nkojap, A.K., Kojom, J.J.W., Stark, T.D., Fouokeng, Y., *et al.* (2023) Rotenoids and Isoflavones from *Xeroderris stuhlmannii* (Taub.) Mendonça & E.P. Souza and Their Biological Activities. *Molecules*, **28**, Article 2846. https://doi.org/10.3390/molecules28062846

[9] Nkojap Kuinze, A., Nguemfo, E.L., Nana Yousseu, W., Wanche Kojom, J.J., Zangueu Bogning, C., Sonfack, C.S., *et al.* (2024) *Xeroderris stuhlmannii* (Taub.) Mendonça & E.P. Sousa (Fabaceae): Evidence of the Antihypertensive and Antioxidant Activities of Its Leaf Aqueous Extract in Cadmium Chloride Hypertensive Rats. *Heliyon*, **10**, e38075. https://doi.org/10.1016/j.heliyon.2024.e38075

[10] Nyathi, B., Bvunzawabaya, J.T., Venissa P Mudawarima, C., Manzombe, E., Tsotsoro, K., Selemani, M.A., *et al.* (2023) Inhibitory and *in Silico* Molecular Docking of *Xeroderris stuhlmannii* (Taub.) Mendonca & E.P. Sousa Phytochemical Compounds on Human α-Glucosidases. *Journal of Ethnopharmacology*, **312**, Article ID: 116501. https://doi.org/10.1016/j.jep.2023.116501

[11] Selemani, M.A., Kazingizi, L.F., Manzombe, E., Bishi, L.Y., Mureya, C., Gwata, T.T., *et al.* (2021) Phytochemical Characterization and *in Vitro* Antibacterial Activity of *Xeroderris stuhlmannii* (Taub.) Mendonca & E.P. Sousa Bark Extracts. *South African Journal of Botany*, **142**, 344-351. https://doi.org/10.1016/j.sajb.2021.07.006

[12] Aarjane, M., Aouidate, A., Slassi, S. and Amine, A. (2020) Synthesis, Antibacterial Evaluation, *in Silico* ADMET and Molecular Docking Studies of New N-Acylhydrazone Derivatives from Acridone. *Arabian Journal of Chemistry*, **13**, 6236-6245. https://doi.org/10.1016/j.arabjc.2020.05.034

[13] Abishad, P., Niveditha, P., Unni, V., Vergis, J., Kurkure, N.V., Chaudhari, S., *et al.* (2021) *In Silico* Molecular Docking and *in Vitro* Antimicrobial Efficacy of Phytochemicals against Multi-Drug-Resistant Enteroaggregative *Escherichia coli* and Non-Typhoidal *Salmonella* spp. *Gut Pathogens*, **13**, Article No. 46. https://doi.org/10.1186/s13099-021-00443-3

[14] Ahmed, A., Saeed, A., Ejaz, S.A., Aziz, M., Hashmi, M.Z., Channar, P.A., *et al.* (2022) Novel Adamantyl Clubbed Iminothiazolidinones as Promising Elastase Inhibitors: Design, Synthesis, Molecular Docking, ADMET and DFT Studies. *RSC Advances*, **12**, 11974-11991. https://doi.org/10.1039/d1ra09318e

[15] Ali, F.T., Yousef, A.K., Ahmed, F.A., Elgneady, F.M., El-Adl, K. and Elhady, M.M. (2022) *In Silico* ADMET, Docking, Anti-Proliferative and Antimicrobial Evaluations of Ethanolic Extract of *Euphorbia dendroides* L. *South African Journal of Botany*, **150**, 607-620. https://doi.org/10.1016/j.sajb.2022.08.009

[16] Aljohny, B.O., Rauf, A., Anwar, Y., Naz, S. and Wadood, A. (2021) Antibacterial, Antifungal, Antioxidant, and Docking Studies of Potential Dinaphthodiospyrols from *Diospyros lotus* Linn Roots. *ACS Omega*, **6**, 5878-5885. https://doi.org/10.1021/acsomega.0c06297

[17] Anza, M., Endale, M., Cardona, L., Cortes, D., Eswaramoorthy, R., Zueco, J., *et al.* (2021) Antimicrobial Activity, *in Silico* Molecular Docking, ADMET and DFT Analysis of Secondary Metabolites from Roots of Three Ethiopian Medicinal Plants. *Advances and Applications in Bioinformatics and Chemistry*, **14**, 117-132. https://doi.org/10.2147/aabc.s323657

[18] de Ruyck, J., Brysbaert, G., Blossey, R. and Lensink, M. (2016) Molecular Docking as a Popular Tool in Drug Design, an *in Silico* Travel. *Advances and Applications in Bioinformatics and Chemistry*, **9**, 1-11. https://doi.org/10.2147/aabc.s105289

[19] Garkusha, N.A., Anikeeva, O.P., Bayıl, I., Taskin-Tok, T. and Safin, D.A. (2023) DFT, ADMET, Molecular Docking and Molecular Dynamics Studies of Pyridoxal. *Journal of the Indian Chemical Society*, **100**, Article ID: 100926. https://doi.org/10.1016/j.jics.2023.100926

[20] Islam, M.D., Saha, J.K., Marufa, S.S., Kundu, T.K., Hossain, I., Nishino, H., *et al.* (2025) Synthesis, Antibacterial Activity, *in Silico* ADMET Prediction, Docking, and Molecular Dynamics Studies of Substituted Phenyl and Furan Ring Containing Thiazole Schiff Base Derivatives. *PLOS ONE*, **20**, e0318999. https://doi.org/10.1371/journal.pone.0318999

[21] Yang, Y., Yao, K., Repasky, M.P., Leswing, K., Abel, R., Shoichet, B.K., *et al.* (2021) Efficient Exploration of Chemical Space with Docking and Deep Learning. *Journal of Chemical Theory and Computation*, **17**, 7106-7119. https://doi.org/10.1021/acs.jctc.1c00810

[22] Friesner, R.A., Murphy, R.B., Repasky, M.P., Frye, L.L., Greenwood, J.R., Halgren, T.A., *et al.* (2006) Extra Precision Glide: Docking and Scoring Incorporating a Model of Hydrophobic Enclosure for Protein-Ligand Complexes. *Journal of Medicinal Chemistry*, **49**, 6177-6196. https://doi.org/10.1021/jm051256o

[23] Lu, C., Wu, C., Ghoreishi, D., Chen, W., Wang, L., Damm, W., *et al.* (2021) OPLS4: Improving Force Field Accuracy on Challenging Regimes of Chemical Space. *Journal of Chemical Theory and Computation*, **17**, 4291-4300. https://doi.org/10.1021/acs.jctc.1c00302

[24] Monk, B.C., Sagatova, A.A., Hosseini, P., Ruma, Y.N., Wilson, R.K. and Keniya, M.V. (2020) Fungal Lanosterol 14α-Demethylase: A Target for Next-Generation Antifungal Design. *Biochimica et Biophysica Acta* (*BBA*)—*Proteins and Proteomics*, **1868**, Article ID: 140206. https://doi.org/10.1016/j.bbapap.2019.02.008

[25] Salman, M., Sharma, P., Kumar, M., Ethayathulla, A.S. and Kaur, P. (2022) Targeting Novel Sites in DNA Gyrase for Development of Anti-Microbials. *Briefings in Functional Genomics*, **22**, 180-194. https://doi.org/10.1093/bfgp/elac029

[26] Hawser, S., Lociuro, S. and Islam, K. (2006) Dihydrofolate Reductase Inhibitors as

Antibacterial Agents. *Biochemical Pharmacology*, **71**, 941-948. https://doi.org/10.1016/j.bcp.2005.10.052

[27] Tsahnang Fofack, H.M., Mbah Bake, M., Petry, S., Ateba, B.A., Amoa Onguéné, P., Mohammad-Salim, H., *et al.* (2024) Identification of Potential Dipeptidyl Peptidase IV Inhibitors from the Conmednp Library by Virtual Screening, and Molecular Dynamics Methods. *Heliyon*, **10**, e35191. https://doi.org/10.1016/j.heliyon.2024.e35191

[28] Lewis, R.J., Singh, O.M., Smith, C.V., Skarzynski, T., Maxwell, A., Wonacott, A.J., *et al.* (1996) The Nature of Inhibition of DNA Gyrase by the Coumarins and the Cyclothialidines Revealed by X-Ray Crystallography. *The EMBO Journal*, **15**, 1412-1420. https://doi.org/10.1002/j.1460-2075.1996.tb00483.x

[29] Mohammed Ameen, S.S., Kh. Ibrahim, M., Chellegui, M., R. Mohammed, S., Mohammad-Salim, H., M. Omer, K., *et al.* (2025) Claisen-Schmidt Synthesis of Azo-Chalcone Catalyzed by a Zinc-Based Metal-Organic Framework: Structural Characterization, Density Functional Theory Calculations, and Molecular Docking Studies. *Reaction Kinetics, Mechanisms and Catalysis*, **138**, 3907-3927. https://doi.org/10.1007/s11144-025-02943-8

[30] Gioia, D., Bertazzo, M., Recanatini, M., Masetti, M. and Cavalli, A. (2017) Dynamic Docking: A Paradigm Shift in Computational Drug Discovery. *Molecules*, **22**, Article 2029. https://doi.org/10.3390/molecules22112029

[31] Genheden, S. and Ryde, U. (2015) The MM/PBSA and MM/GBSA Methods to Estimate Ligand-Binding Affinities. *Expert Opinion on Drug Discovery*, **10**, 449-461. https://doi.org/10.1517/17460441.2015.1032936

[32] Wu, F., Zhou, Y., Li, L., Shen, X., Chen, G., Wang, X., *et al.* (2020) Computational Approaches in Preclinical Studies on Drug Discovery and Development. *Frontiers in Chemistry*, **8**, Article 726. https://doi.org/10.3389/fchem.2020.00726

[33] Sadybekov, A.V. and Katritch, V. (2023) Computational Approaches Streamlining Drug Discovery. *Nature*, **616**, 673-685. https://doi.org/10.1038/s41586-023-05905-z